Chapter 9

POLYMERIC NANOSTRUCTURES

Guojun Liu

Department of Chemistry, University of Calgary, Calgary, Alberta, Canada T2N 1N4

Contents

1. INTRODUCTION

A nanostructure has its smallest dimension in the 1–100-nm size range [1]. Although the size of a polymer coil in dilute solution falls into this range, polymer coils are not considered to be nanostructures because they are structurally not stable (they undergo large-scale

Handbook of Nanostructured Materials and Nanotechnology, edited by H.S. Nalwa
Volume 5: Organics, Polymers, and Biological Materials

ISBN 0-12-513765-6/$30.00

structural fluctuation with time). The radii of surfactant or polymer micelles also fall into the nanometer range. They are not included in the nanostructure category in this chapter because they are not permanent structures either. Micelles form in one solvent and may disintegrate in another. Even in a solvent in which the micelles form, chains are constantly exchanged between micelles and the unimer pool or between different micelles. Polymeric nanostructures in this chapter refer to cross-linked nanometer-sized structures prepared from polymers and, in particular, block copolymers.

A major driving force for the booming activities in the nanoscience and nanotechnology field has been the demand for ever smaller electronic devices [1]. Also, nanometer-sized semiconductors are interesting for their unique properties derived from the quantum size effect. Further interest derives from the expectation that composites made from nanoparticles may be useful as high performance construction materials and that nanoengineered materials may imitate the functions of proteins and enzymes in molecular recognition.

As is evident from this handbook, nanostructures are typically prepared from inorganic or organic precursors. Other than nanosphere preparation from microemulsion [2] or precipitation [3] polymerization, no systematic work has been reported before ours on synthesizing different nanostructures from polymers. For this reason, this chapter will essentially review our work in the past 3–4 years. Results of other groups will be referenced in the sections that discuss the preparation of individual nanostructures.

The scarcity of activities in polymeric nanostructure preparation and study is not in line with the potentially important role polymeric nanostructures may play in future nanometer-sized or molecular electronic devices. A thin polymer film with nanochannels may, for example, be an ideal matrix for semiconductor or metal nanocomponent embedment for preparing nanoelectronic devices just like the use of plastic cards to hold integrated circuits. Also, nanochannels with precisely controlled size and size distribution in thin polymer films can be used as templates for preparing nanomaterials [4] or can be used in separating chemicals with minor size or functionality differences, a function enzyme or protein chemists try to mimic. In the membrane application, the obvious advantage of using a polymer is that one can easily obtain large continuous films. Although hexagonally packed uniform nanochannels can be prepared in individual zeolite particle [5], their preparation in thin films with the channels permeating the whole film thickness is difficult [6].

We prepare nanostructures mostly from block copolymers. A copolymer is a macromolecule that contains two or more types of basic units or monomers. A block copolymer is a linear copolymer in which the different monomers occur in long sequences or blocks. The simplest block copolymer is diblock copolymer $(A)_n(B)_m$, which consists essentially of two linear polymer chains with n units of A and m units of B joined together head to tail. Some diblock copolymers we first synthesized and used in nanostructure fabrication are polystyrene-*block*-poly(2-cinnamoylethyl methacrylate) (PS-*b*-PCEMA), poly(2-cinnamoylethyl methacrylate)-*block*-poly(acrylic acid) (PCEMA-*b*-PAA), poly(*t*-butyl acrylate)-*block*-poly(2-cinnamoylethyl methacrylate) (P*t*BA-*b*-PCEMA), and polyisoprene-*block*-poly(2-cinnamoylethyl methacrylate) (PI-*b*-PCEMA):

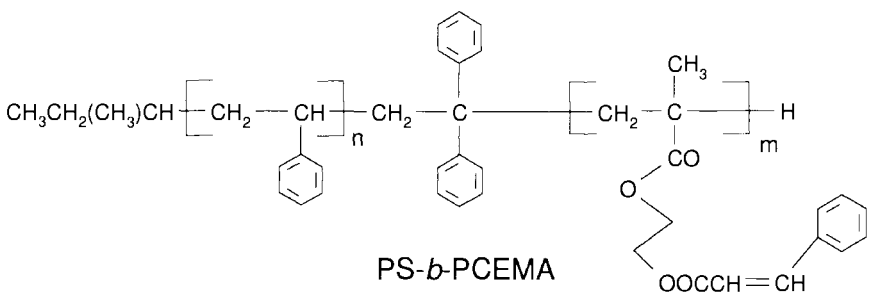

PS-*b*-PCEMA

These block copolymers are unique in that PCEMA is photocross-linkable. Then, the *t*-butyl groups of P*t*BA are easily hydrolyzable and the PI block can be degraded by ozonolysis.

Block copolymers self-assemble under appropriate conditions to form mesophasic structures both in bulk and in solution. In this chapter, a mesophasic structure refers to an uncross-linked precursor to a nanostructure. In a block-selective solvent, a diblock copolymer may, for example, form spherical micelles, where the insoluble block makes up the core and the soluble block forms the corona that stretches into the solution phase [7, 8]. If the PCEMA block of the preceding diblocks forms the core, photolysis of such micelles would yield "permanent" structures, which we refer to as star polymers or hairy nanospheres for micelles with relatively thick or thin corona, respectively. Using the simple strategy of "locking in" mesophasic structure, we prepared a range of nanostructures including star polymers, nanospheres, "tadpole molecules," cross-linked polymer brushes (monolayers), and nanofibers. The nanospheres can be subdivided further into hairy nanospheres (cross-linked nanospheres with polymer chains on their surfaces), shaved nanospheres, nanospheres with cross-linked shells, and hollow nanospheres. In a hairy hollow nanosphere, long hair grows from both the outer and inner surfaces of the solid shell. The hair can be long relative to the size of the inner cavity, but its volume fraction in the cavity should be $\sim$10%. Hairy nanospheres are different from those with cross-linked shells in which the caged chains are densely packed. More sophisticated nanostructures, such as nanochannels in thin films and semi- and fully-shaved hollow nanospheres, were obtained by combining cross-linking with degradation. Semi- and fully-shaved hollow nanospheres were obtained by shaving the outer polymer chains and all of the chains off hairy nanospheres, respectively.

The next section describes the preparation and characteristics of diblocks. The subsequent sections are devoted to discussion of properties and applications of individual nanostructures before some conclusions are drawn in Section 10.

2. POLYMER SYNTHESIS AND CHARACTERIZATION

The precursors to the diblocks containing PCEMA were synthesized by anionic polymerization. To prepare PS-*b*-PCEMA, styrene was polymerized at $-78\,^{\circ}C$ in tetrahydrofuran (THF) using *sec*-butyl lithium as the initiator [9, 10]. Then 1,1-diphenyl ethylene (DPE) and lithium chloride, both at 3 molar equivalents to *sec*-butyl lithium, were added. DPE reacted with polystyryl (PS) anions to convert them into the sterically more hindered PS-DPE anions. Lithium chloride improved the polydispersity of the second block. The second block was prepared by initiating the polymerization of trimethylsiloxyethyl methacrylate (HEMA-TMS) with PS-DPE anions. The trimethylsilyl protecting groups were removed by hydrochloric acid-catalyzed hydrolysis of PS-*b*-P(HEMA-TMS) in a THF/methanol mixture to produce polystyrene-*block*-poly(2-hydroxylethyl methacrylate) (PS-*b*-PHEMA). PS-*b*-PHEMA was then reacted with cinnamoyl chloride in pyridine to attach the cinnamoyl groups.

To synthesize PCEMA-*b*-PAA, HEMA-TMS and *t*-butyl acrylate (*t*BA) were polymerized sequentially with fluorenyl lithium at $-78\,^{\circ}C$ in THF to yield P(HEMA-TMS)-*b*-P*t*BA [11]. P(HEMA-TMS)-*b*-P*t*BA was then hydrolyzed in acidic methanol at room temperature to yield PHEMA-*b*-P*t*BA. After cinnamation of PHEMA in pyridine, the *t*-butyl groups of P*t*BA were removed following the procedure of Jung and Lyster [12].

P*t*BA-*b*-P(HEMA-TMS) was prepared by reversing the polymerization order of HEMA-TMS and *t*BA used for preparing P(HEMA-TMS)-*b*-P*t*BA [13].

To prepare PI-*b*-PCEMA, isoprene was polymerized in a minimal amount of hexane at room temperature for 2 days using *sec*-butyl lithium as the initiator [14]. After the addition

Table I. Important Characteristics of the Polymers Used [19]

Laboratory code	(n/m) by NMR	$\overline{M}_w/\overline{M}_n$ by GPC	$10^{-4}\overline{M}_w$ by GPC	$10^{-4}\overline{M}_w$ by LS	$10^{-2}n$	$10^{-2}m$
			PS-*b*-PCEMA			
S813-C59	13.8	1.17	9.6	10.0	8.1	0.59
S267-C22	12.0	1.10	2.9	3.4	2.7	0.22
S342-C34	10.1	1.14	3.8	4.4	3.4	0.34
S122-C12	9.9	1.13	1.5	1.6	1.22	0.12
S204-C22	9.6	1.09	2.5	2.7	2.04	0.22
S1640-C182	9.0	1.10	21.8	21.8	16.4	1.82
S1209-C152	7.9	1.10	14.8	16.5	12.1	1.52
S750-C107	7.0	1.12	10.0	10.6	7.5	1.07
S859-C268	3.2	1.09	9.7	15.9	8.6	2.7
S1077-C1158	0.93	1.10	24.4	29.6	10.8	11.6
			P*t*BA-*b*-PCEMA			
*t*380-C640	0.59	1.18		22.1	3.8	6.4
			PCEMA-*b*-PAA			
C460-A187	0.41	1.09[a]	5.5[a]	13.3	4.6	1.87
C360-A560	0.65	1.07[a]	6.9[a]	16.6	3.6	5.6
			PI-*b*-PCEMA			
I88-C231	0.38	1.19	2.7	6.6	0.88	2.3
I346-C179	1.94	1.11	2.9	7.0	3.5	1.8

[a] Results obtained for PCEMA-*b*-P*t*BA, precursor to PCEMA-*b*-PAA.

of freshly distilled DPE, THF was introduced into the polymerization flask by cryodistillation. HEMA-TMS was polymerized at $-78\,^{\circ}C$ for 2 h before the polymerization was terminated by methanol.

The polymers synthesized were characterized by gel permeation chromatography (GPC), proton nuclear magnetic resonance (^1H NMR), and light scattering (LS). The important characteristics of the polymers used to prepare the nanostructures described in this chapter are summarized in Table I. For GPC molar mass measurement in THF, the columns were calibrated with monodisperse PS standards.

3. STAR POLYMERS

A star polymer is a macromolecule that consists of three or more linear polymer chains of approximately equal length joined together at one end to a core. The core of a star polymer should be small relative to the size of each arm or constituent polymer chain. A hairy nanosphere consists of a relatively large cross-linked spherical core with a thin corona. Star polymers and hairy nanospheres (see Fig. 1) were prepared by us from essentially the same method by cross-linking the core block of diblock copolymer micelles in a block-

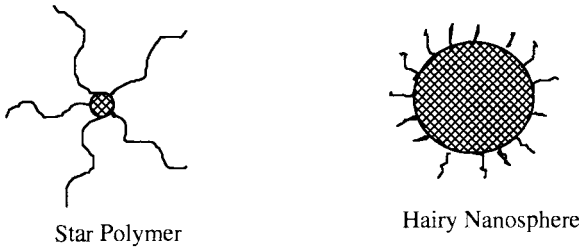

Fig. 1. A star polymer and a hairy nanosphere. (Source: Reprinted with permission from [19]. © 1996 American Chemical Society.)

selective solvent. The difference lies in the use of diblocks with different relative block lengths.

Several groups achieved diblock micelle cross-linking before us. Thermal [15] or photoinitiators [16, 17] were used in these studies to effect the cross-linking of the core block of the diblock micelles. These strategies worked well in the solid state in which the rate of domain fixation was much faster than that of micelle chain exchange [18]. In solution, insoluble products were sometimes obtained due to micelle fusion during core cross-linking [15]. PCEMA photocross-linked without additives such as an initiator. Using diblocks containing PCEMA, soluble star polymers [19, 20] and hairy nanospheres [11, 19] were always prepared.

3.1. Example Preparation

Micelles were prepared by refluxing S813-C59 (Table I, i.e., a PS-*b*-PCEMA sample with 8.1×10^2 units of styrene and 59 units of CEMA) in cyclopentane (CP; 95%, Aldrich) for 2 days. The sample was then photolyzed with UV light from a 500-W mercury lamp that had passed through a 260-nm cutoff filter to achieve a CEMA conversion of 40%. The sample was then collected by precipitation into methanol. Illustrated in Figure 2 is a transmission electron microscope (TEM) image of the star polymer prepared from S813-C59. Because the sample was stained by OsO_4, which selectively reacted with the residual aliphatic double bonds in PCEMA, the PCEMA region appears dark. Figure 2 clearly shows that PCEMA makes up the core and PS constitutes the relatively thick gray shell of the micelles, as expected. Also, the star polymer appears to have a relatively narrow size distribution, as confirmed by both GPC and dynamic light scattering results. Molar mass determination showed that this polymer had 115 arms.

S813-C59 had a n/m value of 13.8. It should be possible to increase the n/m value to minimize the relative CEMA content in the cross-linked micelles. At even larger n/m values, the cross-linked micelles are essentially star polymers.

3.2. Robustness of This Method

There are several traditional methods for star polymer preparation [21]. Our method is unique for its robustness in producing star polymers with a large number of arms. For example, with this method we prepared a star polymer with 2.0×10^3 arms and a molar mass of 9.0×10^8 g/mol [22].

Also, the PS and PCEMA blocks were found to phase-segregate well in the star polymers, and the star polymers prepared generally had narrow size distributions. Determination of the size and molar mass of PS-*b*-PCEMA micelles in cyclopentane before and after UV irradiation indicated that the photocross-linking locked in only the micellar structure and did not change the aggregation number of the micelles [20].

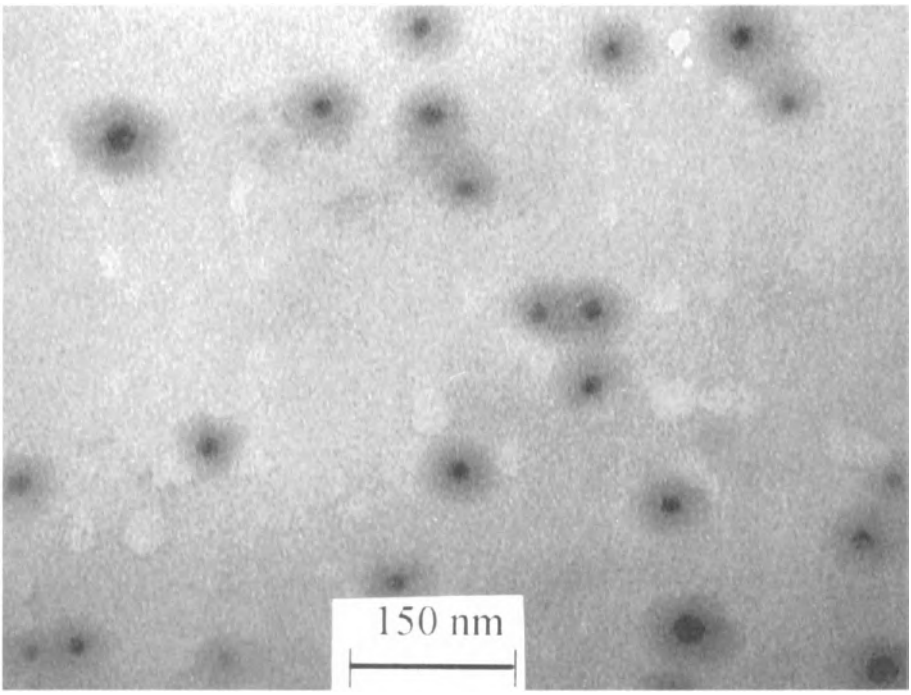

Fig. 2. TEM image of cross-linked S813-C59 micelles. (Source: Reprinted with permission from [20]. © 1997 American Chemical Society.)

3.3. Applications

Star polymers are useful in industry as melt strength improvers. We carried out some fundamental studies of PS-*b*-PCEMA micelles by taking advantage of the "locking in" feature of the micelle photocross-linking process. Assuming the star (thick corona and small core) and crew-cut (large core and thin corona) micelle models, Halperin [23] and de Gennes [24] derived the scaling relationship for aggregation number, f, of diblock micelles formed in a block-selective solvent,

$$f \approx m^{\alpha} \tag{1}$$

where m is the number of repeat units in the insoluble block. For star micelles, $\alpha = 0.80$. This value increases to 1 for crewcut micelles.

Aggregation numbers, f, were reported as a function of m for several systems [25–32]. Except in one system [32], the m dependence of f did not follow Eq. (1) at all. The reason for the discrepancy between the theory and experimental results varied from system to system. In some cases, abrupt increases in f with m were observed, probably due to the formation of cylindrical or vesicular micelles instead of spherical micelles as m changed. Other systems probably never reached thermodynamic equilibrium.

We examined the m dependence of f for micelles prepared from the first six PS-*b*-PCEMA diblocks in Table I [20]. The diblocks were refluxed in cyclopentane for 2–3 days to ensure micellar structure equilibrium before they were photolyzed at 50 °C to yield star polymers. TEM was used to confirm the spherical shape of the micelles. Taking advantage of the "permanent" nature of the star polymers, we separated unimers from the star polymers by GPC fractionation. The molar masses of the stars were determined in toluene at room temperature by light scattering. Plotted in Figure 3 is $\ln f$ vs. $\ln m$ for the six star polymers. The slope obtained from linear regression was $\alpha = 0.92$ with a correlation coefficient of 0.975 [20]. Although the data quality as judged from the correlation coeffi-

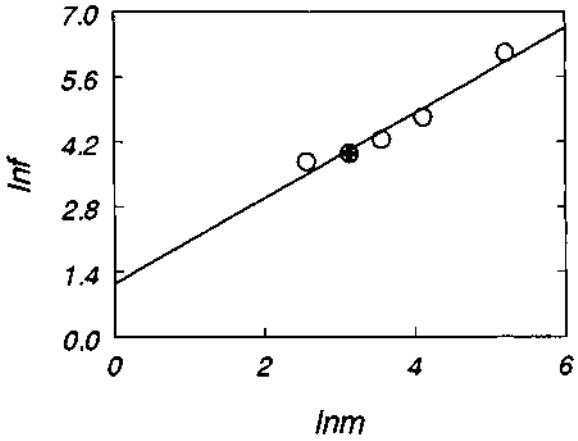

Fig. 3. Plot of ln f vs. ln m for six PS-*b*-PCEMA star polymers. The plus sign represents the S267-C22 datum that overlaps with that of S267-C22.

cient is still poor, it represents a great improvement over the correlation coefficient of 0.86 obtained by Khougaz et al. [32] for another system. Also, the α value is between those predicted by Halperin [23] and by de Gennes [24]. Thus, the scaling results appear correct. As to which model is more appropriate, a further study involving samples with a larger m range is being carried out.

The advantages offered by micelle cross-linking in this study are twofold. First, the f value can be determined more accurately because of the separation of the star polymers from the unimers. Then, light scattering studies of the star polymers can be carried out at room temperature in toluene or any other good solvents for PS instead of at 50 °C in cyclopentane in which the micelles were prepared. It was inconvenient to use cyclopentane for light scattering measurements because the purest commercial cyclopentane is only 95% pure. To determine the specific refractive index increment (required for molar mass evaluation) in a mixed solvent, one has to dialyze a polymer solution against the solvent. This is a tedious process.

4. HAIRY NANOSPHERES

4.1. Example Preparation

We prepared hairy nanospheres from PS-*b*-PCEMA with short PS and long PCEMA blocks [19]. The preparation of nanospheres from PCEMA-*b*-PAA is described here because these nanospheres are water soluble and may be more useful. C460-A187 (PCEMA-*b*-PAA with 4.6×10^2 units of CEMA, 187 units of acrylic acid, and a PAA weight fraction of 10%) was dissolved in dimethylformamide (DMF) [11]. Water was added dropwise until it reached a volume fraction of 80%. The mixture was then dialyzed against distilled water for 4 days to remove DMF. Permanent PCEMA nanospheres were obtained after UV irradiation of the crewcut micelles.

A TEM photograph of some nanospheres prepared from this polymer is shown in Figure 4. The cross-linked micelles are spherical and have a narrow size distribution around a mean diameter of ~25 nm. These probably represent cross-linked spheres of this size with the narrowest size distribution, because microemulsion polymerization has been known not to work well in producing spheres with diameters smaller than 100 nm with narrow size distributions [2].

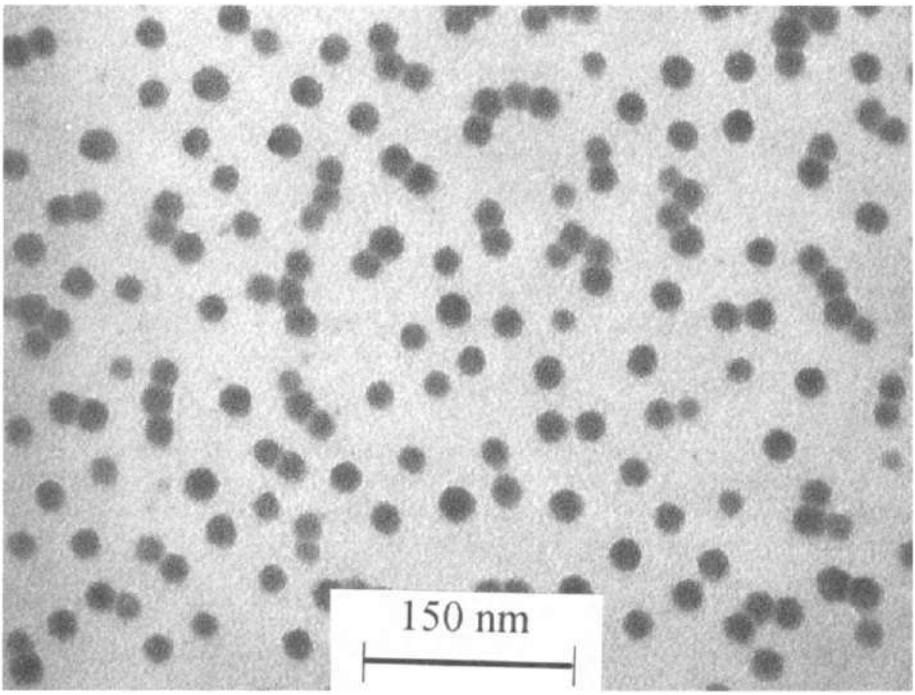

Fig. 4. TEM image of C460-A187 nanospheres.

Although also stained with OsO_4, the nanospheres do not show a distinctive PAA layer. This is in agreement with the hairy nanosphere picture in which the corona is thin relative to the core.

More recently, C360-A560 was used to prepare nanospheres [33, 34]. Whereas the PAA block is relatively long in this diblock, which makes the polymer directly soluble in warm water, the use of DMF and the dialysis step were thus unnecessary.

4.2. Properties of the Nanospheres and Potential Applications

PCEMA-*b*-PAA nanospheres possess hydrophobic PCEMA cores and a hydrophilic PAA corona. The core can uptake a lot of organic compound from water. The hydrodynamic radius, R_h, of 48 nm for the C460-A187 nanospheres in water, for example, increased to 62 nm in water/DMSO (dimethyl sulfoxide) with 2.5% DMSO by volume [12]. This represents a nanosphere volume increase of 116% due to DMSO uptake.

The nanospheres can also uptake solid organic compounds from water [33, 34]. In one experiment, solid perylene was stirred with 4.00 mL of a C360-A560 nanosphere solution at 6.8×10^{-2} mg/mL for 3 weeks. The excess solid perylene was then filtered out and the amount of perylene incorporated into the nanospheres was analyzed by monitoring the fluorescence intensity from the supernatant. Plotted in Figure 5 is the increase in the perylene fluorescence intensity as a function of the amount of solid perylene, m_{PE}, added initially to the aqueous nanosphere solution. The fluorescence intensity initially increases steeply with m_{PE}. The rate of perylene fluorescence intensity increase with m_{PE} decreases at greater m_{PE} values and the intensity value eventually levels off.

The initial fluorescence intensity increase with m_{PE} is expected because the amount of perylene solubilized into the nanosphere cores (perylene solubility in water is very low) increases with m_{PE}. The leveling off of the fluorescence intensity at high m_{PE} is reasonable as well. The nanospheres have only a certain capacity. Once saturated, they cannot uptake more perylene, regardless of how much perylene is added. The excess perylene in

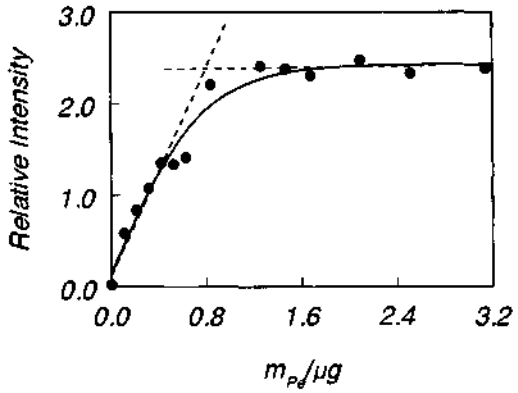

Fig. 5. Increase in perylene fluorescence intensity as a function of the amount of perylene added, m_{P_E}, to 4.00 mL of a C360-A560 nanosphere solution at a concentration of 6.8×10^{-2} mg/mL.

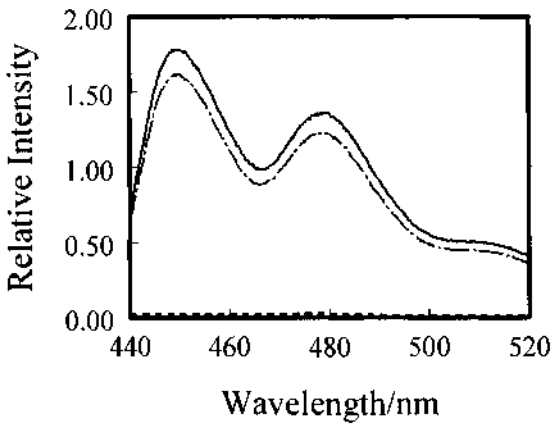

Fig. 6. Comparison of the perylene fluorescence spectra of a 2.50-mL perylene-saturated C360-A560 nanosphere solution at a concentration of 6.8×10^{-2} mg/mL (—), after the addition of 80 μL of a 0.100-M $CaCl_2$ solution (---), and after the addition 120 μL of a 0.100-M EDTA solution (— · —).

the form of microcrystals in the water was removed by filtration and did not contribute to further fluorescence intensity increase. At the intermediate stage, the fluorescence intensity increased more slowly with m_{PE}, possibly for two reasons. First, the uptake of many perylene molecules by the same nanosphere may decrease perylene fluorescence quantum yield due to "concentration quenching" or excimer formation. Second, the partition coefficient K of the nanospheres may decrease at higher perylene loadings.

Also illustrated in Figure 5 is our method for determining the capacity of the nanospheres. The maximal amount of perylene the nanospheres can uptake is determined to be 0.77 μg from the crossing point between the straight lines describing intensity vs. m_{PE} data at high and low perylene loadings. Because the total amount of nanospheres used was 0.272 mg, the capacity of the nanospheres is 2.83 mg/g.

This trapping capacity is disappointingly low. The value was increased to ~300 mg/g by stirring an aqueous nanosphere solution with perylene in the presence of some acetone. Acetone helped increase the trapping capacity, probably because acetone swelled the PCEMA core, which facilitated the penetration of the core by perylene, a molecule with five fused benzene rings.

We then demonstrated that the perylene-loaded nanospheres could be precipitated out by the addition of $CaCl_2$ to the calcium concentration of $\sim 2.0 \times 10^{-3}$ M (Fig. 6). Ca^{2+}

caused the precipitation of the nanospheres, probably by the bonding of each Ca^{2+} cation with two AA units from different nanospheres.

The precipitated nanospheres were then extracted with an organic solvent such as THF to remove the perylene. Once perylene was removed, the nanospheres could be redispersed in water by adding sodium carbonate to precipitate Ca^{2+} or by adding ethylenediamine tetraacetate (EDTA) to complex with Ca^{2+} (Fig. 6).

Based on these observations, we believe that the nanospheres should be useful in cleaning up tailings ponds left behind by the oil and gas industry. In such ponds, the relatively low molar mass hydrocarbons should function to plasticize the core of the nanospheres. The plasticized nanospheres should be able to uptake a large amount of high molar mass components such as asphalt. In addition, the nanospheres may be useful as drug carriers in controlled drug release.

Other than the trapping capacity study, we also determined the coefficient of perylene partition between water and PCEMA-*b*-PAA nanosphere cores to be 3.3×10^5 by using a fluorescence method. This figure suggests that perylene is 3.3×10^5 times more likely to reside inside the nanosphere cores than in water at an equal nanosphere core and water volume. We also studied perylene uptake kinetics. In all cases, the perylene partition equilibrium was established within 2 days [33, 34].

5. TADPOLE MOLECULES

So far, the photocross-linking of micelles to produce star polymers and nanospheres has been discussed. Coexisting with micelles are some unimers or unimolecular micelles. In a unimer, the insoluble block should cluster together like a globule and the soluble block should assume the normal random coil conformation, as first hypothesized by Sadron [35].

An indirect way to verify the unimer shape is to show that a diblock shrinks in size in a block-selective solvent. This verification has been difficult, because the critical micelle concentration of a diblock is normally too low to allow the use of scattering techniques to determine the unimer size in a block-selective solvent.

This difficulty was circumvented by using PS-*b*-PCEMA. When photolyzed in a block-selective solvent, not only micelle but also unimer structures are locked in. An intramolecularly cross-linked unimer should have a globular PCEMA head and a PS tail, and structurally resembles a tadpole. The structurally stable tadpole molecules and cross-linked micelles then can be separated by fractionation precipitation or GPC. Light scattering studies of the tadpoles can be performed in any solvents in which the tadpoles are soluble.

5.1. Example Preparation

S859-C268 was dissolved in THF [36]. Cyclopentane (CP) was added to a CP volume fraction of 60%. Such a solution was photolyzed to give a CEMA conversion of 26%. The tadpole molecules were then separated from the cross-linked micelles by GPC fractionation. Light scattering studies of the tadpoles in toluene gave a radius of gyration of 14.2 ± 1.0 nm and a molar mass of $(1.59 \pm 0.22) \times 10^5$ g/mol; those for the diblock were 19.1 ± 0.7 nm and $(1.65 \pm 0.07) \times 10^5$ g/mol. Although the tadpole molecules have the same molar mass as the diblock within experimental error, the decrease in size suggests the tadpole shape of the intramolecularly cross-linked unimers and the retention of the tadpole shape in toluene.

5.2. Some Future Prospects

This study represents the first preparation and isolation of diblock tadpole molecules. They may have unique diffusional properties. It remains to be seen how the properties of the

cross-linked block of the tadpoles differ from those of the molecular globules prepared from intracross-linking linear homopolymers at high dilutions [37].

6. HOLLOW NANOSPHERES

Other than spherical micelles, block copolymers also can form vesicular [14, 38, 39], cylindrical [20, 38–40], and donut-shaped micelles [39] in block-selective solvents. The exact morphology of the micelles formed depends on the n/m value of the diblock and the composition of the binary mixture used as the solvent [38, 39]. In general, diblocks with a short soluble and long insoluble block tend to form vesicles, cylinders, or donuts. Increasing the content of the block-selective solvent relative to the mutual solvent for both blocks may induce vesicle, cylinder, or donut formation in a binary solvent mixture. A block-selective solvent and mutual solvent for PS-*b*-PCEMA are, for example, CP and THF, respectively.

Copolymer I88-C231 has a low PI weight fraction and formed vesicles in THF/hexanes (HX) with HX volume fractions greater than 50%. In such a vesicle, the insoluble PCEMA block makes up the essentially solvent-free shell. The soluble PI block stretches into the solution phase from both the inner and outer surfaces of the shell. Hairy hollow nanospheres were prepared by photocross-linking the PCEMA shell. Because isoprene was polymerized in hexane using *sec*-butyl lithium as the initiator, 93% of the isoprene units were incorporated into the polymer by 4,1-addition [14]. The double bonds in the backbone of PI were decomposed by ozonolysis to cause PI degradation. Semishaved hollow nanospheres were obtained by selectively cleaving off the outer PI chains. Fully-shaved nanospheres were obtained by removing all the PI chains.

6.1. Example Preparation of Hairy Hollow Nanospheres

I88-C231 was dissolved in THF/HX with 35% HX by volume. The solution was then slowly added into an equal volume of THF/HX with 85% HX to induce vesicle formation. The vesicle solution in THF/HX with 60% HX was stirred for 1–2 weeks before an equal volume of HX was added to yield a vesicle solution at a concentration of ~1.0 mg/mL in THF/HX with 80% HX. The solution was irradiated immediately to obtain a PCEMA conversion of 40%. The vesicles initially were equilibrated in THF/HX with 60% HX, because the vesicles were found to have the narrowest size distribution at this solvent composition. More HX was added just before irradiation. This supposedly increased the rigidity of the PCEMA shell (due to the reduced PCEMA swelling by THF) and should have decreased intervesicle fusion during the cross-linking process.

Illustrated in Figure 7 is a TEM image of the cross-linked I88-C231 vesicles or hairy nanospheres [41]. The light circle in the center of each particle corresponds to the location of the cavity. The dark ring separating the shell from the cavity represents the inner PI chains, which should have collapsed upon solvent evaporation. The outer PI layer is not evident here because it might be too thin.

6.2. Example Preparation of Semi- and Fully-Shaved Hollow Nanospheres

Hairy hollow nanospheres of I88-C231 were dissolved in methylene chloride and chilled to $-40\,^{\circ}C$. Ozone was bubbled through this solution for $\frac{1}{2}$ or 10 min, depending on whether semi- or fully-shaved hollow nanospheres were prepared. The ozonides formed were then reduced with $P(OCH_3)_3$. Illustrated in Figure 8 is a TEM image of hairy hollow nanospheres treated with O_3 for $\frac{1}{2}$ min. Compared to vesicles of Figure 7, the outer boundaries of the vesicles here are not as sharp, which suggests the degradation of the outer PI layer. The remnants of dark rings at the cavity and shell interfaces indicate the

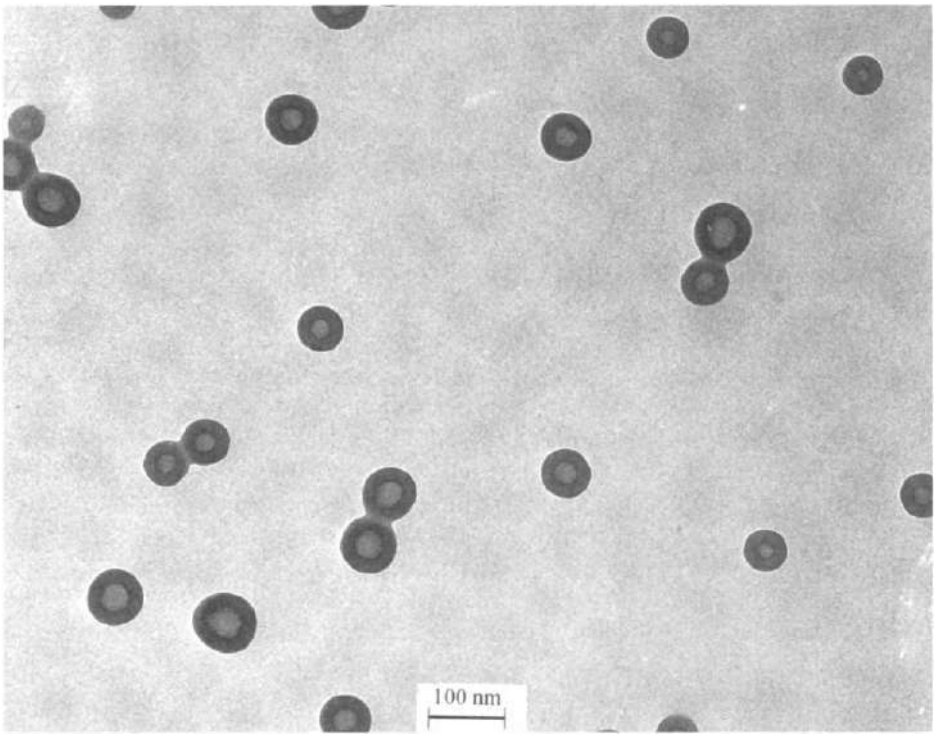

Fig. 7. TEM image of cross-linked 188-C231 vesicles prepared in THF/hexanes with 80% hexanes.

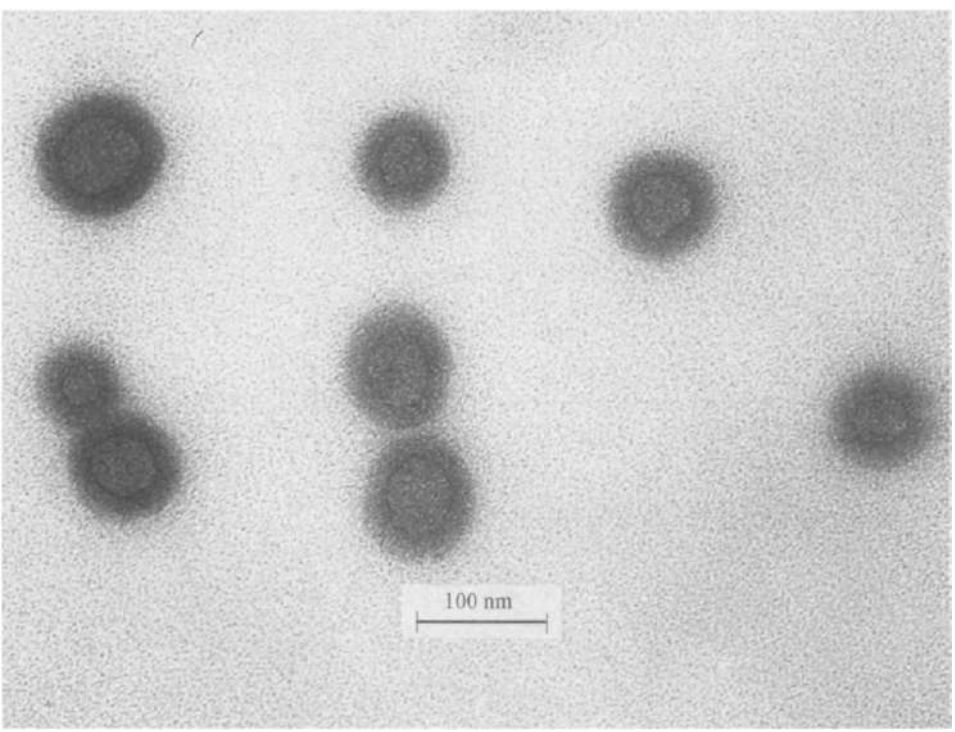

Fig. 8. TEM image of cross-linked 188-C231 vesicles treated with ozone for 0.5 min.

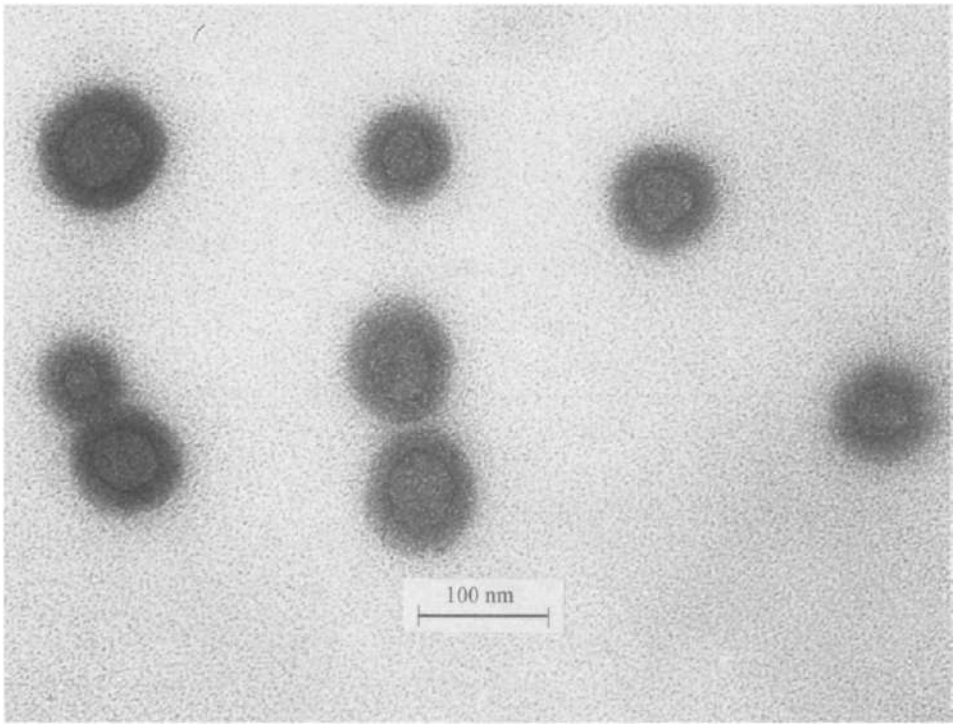

Fig. 9. TEM image of cross-linked I88-C231 vesicles treated with ozone for 10 min.

integrity of the inner PI layer. These conclusions were further substantiated by Fourier transform infrared (FTIR) spectroscopy and light scattering results. Our FTIR results indicated that approximately half of the PI double bonds disappeared after the ozonolysis treatment. A dynamic light scattering study witnessed an 11-nm decrease in the vesicle hydrodynamic radius in THF after the ozonolysis [41].

Illustrated in Figure 9 is a TEM image of some hairy nanospheres treated with ozone for 10 min. The dark ring between the shell and the cavity is absent for the vesicles in Figure 9. This clearly suggests the decomposition of the inner PI layer. This conclusion was confirmed by our FTIR result [41].

6.3. Potential Applications and Some Future Prospects

Semi- and fully-shaved hollow nanospheres were stably dispersed in CH_2Cl_2 after their preparation. Once precipitated and dried, semishaved hollow nanospheres are barely soluble in any organic solvent. The solubility of fully-shaved hollow nanospheres decreases even further. Due to the cavity present in each nanosphere and the voids between different nanospheres in the solid state, these nanospheres may be useful as macroporous resins.

Although selective PI chain degradation was used to demonstrate the superior control in nanoengineering in this study, different chemistry can, in principle, be performed on the inner and outer PI chains to create useful hollow nanospheres. The double bonds of the PI chains on the outer surfaces can, for example, be selectively converted to hydroxyl groups, while the inner PI chains are left intact. If successful, this will yield water-soluble nanospheres with cavities partially filled with PI chains. Whereas the cavities are large (~28 nm in diameter), these species may function as high-capacity absorbents for organic compounds from water. By tailor-making the diblocks, the vesicles also may be used in controlled drug delivery.

6.4. Related Chemistry

Due to the relatively long PI block, I346-C179 formed spherical micelles in THF/HX with HX contents between ~60 and ~95%. Hairy nanospheres were prepared from this diblock by photocross-linking the PCEMA cores. After ozonolysis, the PI block was degraded to yield cross-linked PCEMA nanospheres with immediately attached carbonyl or ketone groups [42]. We have demonstrated that the carbonyl or ketone groups react with a range of reagents such as cyclopentadiene [42] and 2,5-bis(trifluoromethyl)aniline [43]. Although the carbonyl- or ketone-covered nanospheres were not soluble in any organic solvent tested, the nanospheres surface-modified by reaction with cyclopentadiene and 2,5-bis(trifluoromethyl)aniline dissolved in solvents such as hot DMSO. These shaved nanospheres are potentially useful as catalyst supports or as solid lubricants.

7. POLYMER BRUSHES

So far, the preparation of various nanostructures in solution has been discussed. Next, the preparation of diblock brushes or monolayers at the solution and solid interface will be reviewed.

In a block-selective solvent, a diblock copolymer may also be deposited from the solvent and self-assemble to form a polymeric monolayer on a substrate being contacted. If the interaction between the insoluble block and the substrate is favorable, a dense monolayer called a polymer "brush" may form in which the insoluble block spreads on the solid substrate like a melt and the soluble block stretches into the solution phase like bristles of a brush as illustrated in Figure 10 [44–46].

Polymer brushes have been traditionally used to help disperse latex and pigment particles in paint [47]. Due to its industrial relevance, there have been many studies of polymer brushes in the past decade [44–46]. In most previous studies, dilute block copolymer solutions (<0.1%) in which polymer chains existed as unimolecular micelles or unimers were used to coat solid substrates. In such solutions, the soluble block was shown to stretch by the surface-force technique [44, 48–51]. The layered structure (i.e., that the soluble block overlays the insoluble anchoring block) of diblock brushes has been confirmed by surface tension [52] and surface-enhanced Raman scattering (SERS) studies [53–55]. The equilibrium surface coverage of diblocks with different block lengths under otherwise identical conditions [56–59] has been found to follow a scaling relationship derived by Marques et al. [60] for unimer adsorption in the van der Waals buoy regime.

In industrial situations, diblock adsorption occurs in concentrated solutions in which diblock copolymers exist as micelles. We were the first to study polymer brush formation systematically under these conditions [61]. We examined the effect of solvent composition change on brush formation and established different scaling relationships followed by polystyrene-*block*-poly(2-cinnamoylethyl methacrylate) (PS-*b*-PCEMA) adsorption from micellar solutions [9, 62, 63]. From surface-enhanced Raman scattering and TEM studies, we also established that the brushes probably formed due to the disintegration of adsorbed PS-*b*-PCEMA micelles on silica or silver [64]. In this section, only an example preparation

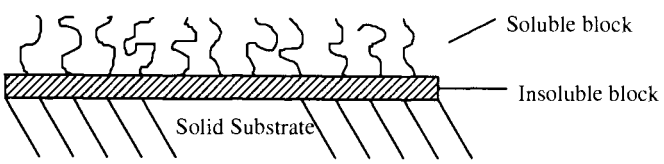

Fig. 10. Illustration of a polymer brush. Reprinted with permission from J. Tao, A. Guo, and G. Liu, *Macromolecules* 29, 1618 (1996).

of cross-linked PS-*b*-PCEMA brushes and TEM evidence for the layered structure of the brush will be shown.

7.1. Example Preparation of Cross-Linked PS-*b*-PCEMA Brushes

S1077-C1158 was dissolved in THF. Cyclopentane was added to a CP content of 82% and a polymer concentration of ~15 mg/mL. Aerosil OX 50 (15 mg; nonporous spherical silica with a specific surface area of 50 m^2/g) was equilibrated with 4.00 mL of this micellar solution for 7 days and separated from the coating solution by centrifugation. The coated silica was then rinsed in fresh THF/CP with 82% CP and precipitated by centrifugation. This process was repeated. The silica particles again were redispersed in the solvent mixture before they were irradiated to a CEMA conversion of 26%. The silica particles could be rinsed in fresh solvent before crosslinking to remove the polymer in the solution phase, because the brush layer was stable in THF/CP with 82% CP, the mixture used for preparing the coating solution.

7.2. Layered Structure of PS-*b*-PCEMA Brushes

Illustrated in Figure 11 is a TEM image of a silica particle coated as described. Because the silica particle was not stained, the inner dark circle must correspond to the silica particle and the outer gray shell represents the polymer layer. Averaging the thickness of the polymer layer over ~20 silica particles yielded a thickness of 29 nm with a standard deviation of 3.7 nm. The average thickness of 29 nm agrees well with 27 nm, calculated from the surface coverage, that is, the amount of polymer adsorbed on a unit silica surface area, determined from an independent experiment.

The brush-coated silica particles were then stained with OsO_4. This increased the diameter of the dark inner circle and decreased the thickness of the gray shell (Fig. 12). Whereas PCEMA should react selectively with OsO_4, the increase in the diameter of the dark inner circle suggests that PCEMA was next to silica. The remnants of a gray polymer layer after staining is in agreement with the picture that PS and PCEMA phase-separated well and PS overlaid the PCEMA layer. Averaging the PS layer thickness over 10 stained silica particles gave a PS layer thickness of 11 nm. This agrees with the expected 7 nm, because PS chains might have partially retained the swollen configuration they assumed in cyclopentane before the particles were sprayed on Formvar-covered copper grids for viewing by TEM. Thus, adsorbed PS-*b*-PCEMA had the brush conformation in THF/CP with 82% CP.

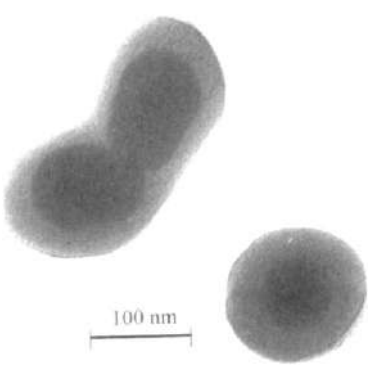

Fig. 11. TEM image of single and fused silica particles coated with S1077-C1158 in THF/CP with 82% CP before OsO_4 staining. (Source: Reprinted with permission from [64]. © 1997 American Chemical Society.)

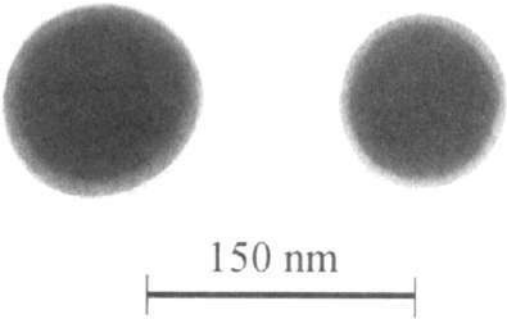

Fig. 12. TEM image of a silica particle coated with S1077-C1158 in THF/CP with 82% CP after OsO_4 staining. (Source: Reprinted with permission from [64]. © 1997 American Chemical Society.)

Also shown in Figure 11 is a brush-covered silica particle aggregate. The image clearly shows the formation of a brush layer at a site with a large surface curvature change. Also the contour of the substrate is approximately mapped by the brush layer.

7.3. Properties and Potential Applications

Cross-linked polymer brushes were resistant to solvent dissolution. This was obvious from our TEM results (see Fig. 11). Before photolysis, S1077-C1158-coated silica particles could not be dispersed in THF. TEM analysis of the precipitated silica particles indicated that the S1077-C1158 layer was removed due to dissolution in THF. On the other hand, TEM analysis showed that the brush was intact after the immersion of the silica particles caged in cross-linked PS-*b*-PCEMA brushes. This explains why the photolyzed PS-*b*-PCEMA-covered silica particles could be dispersed in THF and the resultant dispersion remained stable for days. The stability derived from the steric stabilization effect of the cross-linked polymer brush.

Polymer brush formation is a self-assembling process. To coat a substrate, one needs only to equilibrate the substrate with a polymer coating solution. Due to its convenience, there may be many applications of this process. It can, for example, be used to modify the surface properties of medical devices or to coat silica particles as high-performance liquid chromatography (HPLC) column packing. Also, silica particles caged in cross-linked polymer brushes may be used as plastic fillers [65].

8. BLOCK COPOLYMER NANOFIBERS

The preparation of nanostructures in solution or at a solution/substrate interface has been discussed so far. Next, the preparation of nanostructures starting from solid polymers and the preparation of nanofibers will be addressed.

A nanofiber is a fiber with a nanometer-sized diameter. Nanofibers have been prepared previously mostly from inorganic or organic precursors through the template method. Nanorods [66, 67] were, for example, prepared by filling carbon or boron carbide nanotubes [68, 69] with metal oxides at elevated temperatures. Other templates include the cylindrical pores in a polymer membrane or in anodized alumina [4]. More recently, "soft templates" such as reverse micelles have been used for inorganic nanofiber or nanorod preparation [70]. In addition to the template method, carbon nanofibers have been prepared at particular crystal faces due to the decomposition of selected hydrocarbons [71]. Using Ni nanoparticles as the catalyst, the decomposition of trichloromethyl silane at high temperatures enabled the preparation of SiC nanowhiskers [72].

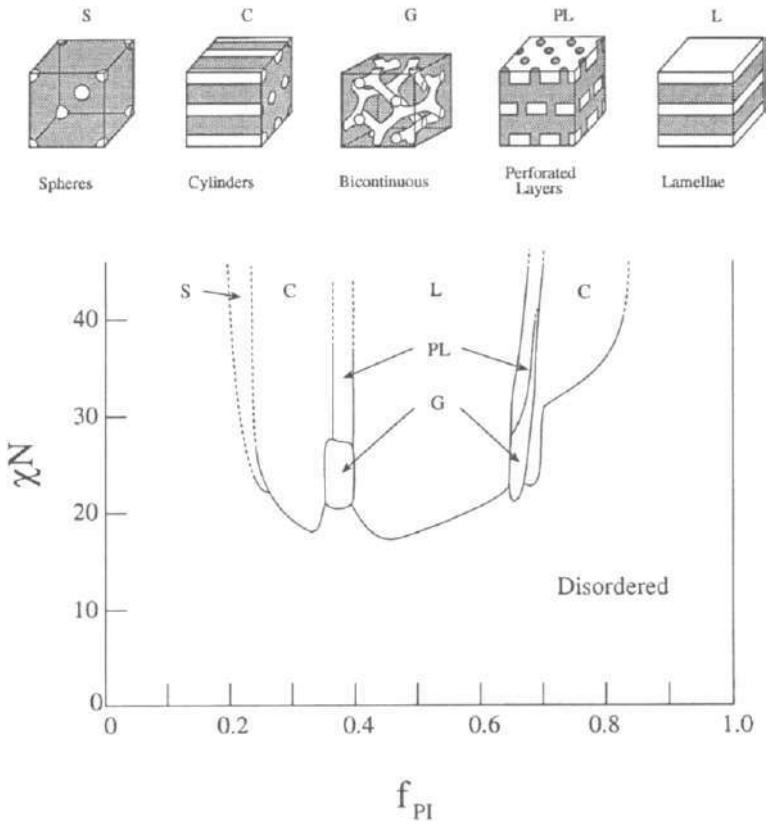

Fig. 13. In the weakly segregated regime ($20 < N\chi < 30$), the PI microdomain (denoted by the white regions) in PS-*b*-PI changes from spherical to cylindrical, gyroidal, and lamellar as the PI volume fraction, f_{PI}, increases to ~50%. At higher molar masses (larger N) and lower temperatures (larger χ), the gyroidal morphology may be replaced by a perforated layer morphology. (Source: Reprinted with permission from [76a]. © 1995 American Chemical Society.)

We prepared the first polymeric nanofiber sample from S750-C107 by taking advantage of the self-organizing properties of the diblock in bulk [73]. Due to the large number of repeat units in a polymer, a minor difference in the properties of two monomers can lead to totally different characteristics in the polymers. This accounts for the incompatibility or immiscibility of most polymers in bulk. Similarly, the A and B blocks of $(A)_n(B)_m$ are incompatible and they segregate from one another in bulk. Due to the bonding between the A and B blocks, they cannot undergo large-scale phase separation. Instead, the size of the segregated A or B domain is similar to that of the individual A or B coil, that is, on the nanometer scale. The domain shape of A or B varies with the diblock composition or the relative n and m values and the temperature [74, 75]. Illustrated in Figure 13 is an experimentally established phase diagram for low molar mass PS-*b*-PI samples [76], where N equals $n + m$ and χ is the styrene–isoprene segment–segment (Flory–Huggins) interaction parameter. The χ parameter for a diblock normally has the temperature, T, dependence $\chi = \alpha/T + \beta$, where α and β are constants for a given polymer and $\alpha > 0$. According to this diagram, PS-*b*-PI in the weakly phase-segregated regime ($20 < N\chi < 30$) is in a disordered state at low PI volume fractions, f_{PI}, or the PI and PS chains are miscible. The PI domains (white regions) may subsequently assume the spherical (S), cylindrical (C), gyroidal (G), and lamellar shape as f_{PI} gradually increases to ~50%. For higher molar mass samples (N larger) or at lower temperatures (χ larger), the gyroidal morphology of the sample may be replaced by a perforated layer morphology. To prepare PS-*b*-PCEMA

nanofibers, the PS-*b*-PCEMA sample we used had a PCEMA weight fraction of 24%, and PCEMA existed as cylinders dispersed in the PS matrix. Photolysis of such a solid sample cross-linked the PCEMA cylinders. Separating different cylindrical domains by dissolving the PS chains yielded nanofibers.

8.1. Example Preparation

Solvent evaporated from a 5-mL S750-C107 solution in toluene, at ~10% by volume, in a polyethylene bottle over a 3–4-day period. The resultant S750-C107 film was dried and annealed under 30-cm Hg pressure at 65 ± 5 °C for 3 days and 105 °C for 2–3 weeks. The film was then irradiated with light from a 500-W mercury lamp that had passed through a 310-nm cutoff filter to obtain a CEMA conversion of ~30%. Dissolution of the resultant film in THF yielded nanofibers as illustrated in the TEM image shown in Figure 14. The nanofibers have a diameter of ~50 nm and length of ~20 μm. The expected PCEMA core and PS shell structure is seen in Figure 15.

The formation of PCEMA cylinders in bulk S750-C107 is evident from Figure 16. This picture was taken of a microtomed and OsO_4-stained specimen before UV irradiation. The dark circles represent PCEMA cylinders pointing out of the picture. The cylinders are packed with the expected hexagonal symmetry.

Other than locking in the cylindrical domains of a bulk sample to produce nanofibers, we observed cylindrical micelle formation from S750-C107 in cyclopentane [20]. The photocross-linking of the PCEMA cores led to the preparation of nanofibers in solution. Fibers prepared this way were, however, not as long as those derived by cross-linking a solid sample. Also, spherical micelles were found to coexist with the cylindrical micelles.

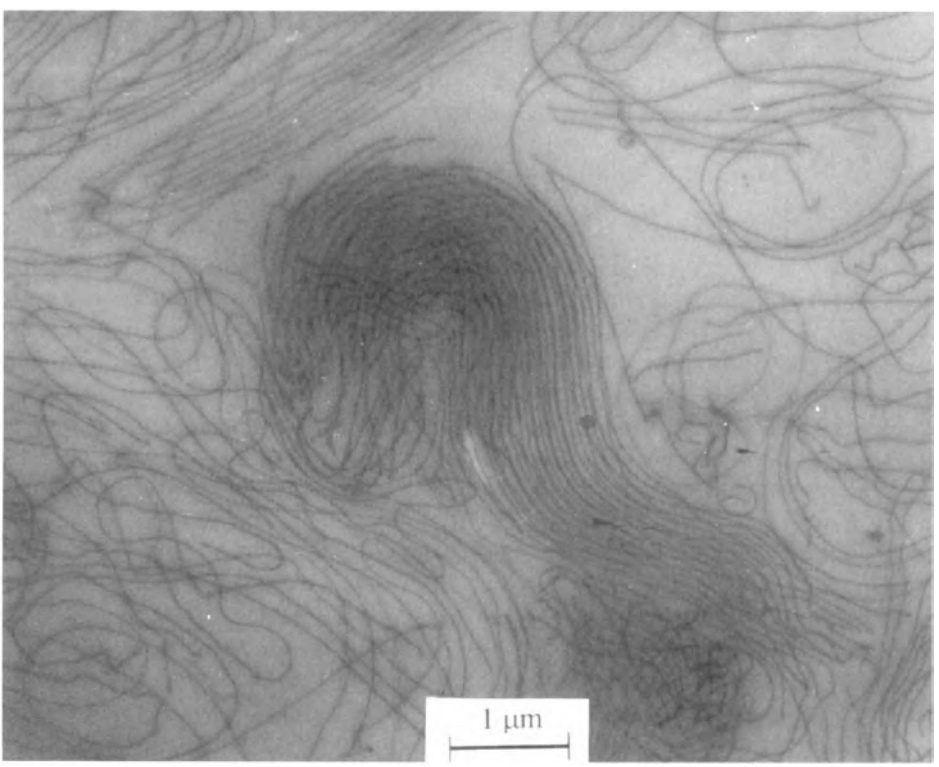

Fig. 14. TEM image of S750-C107 nanofibers. The TEM sample was prepared by transferring a thin film, formed after dispensing a drop of a THF nanofiber solution on a water surface, onto a copper grid. (Source: Reprinted with permission from [73]. © 1996 American Chemical Society.)

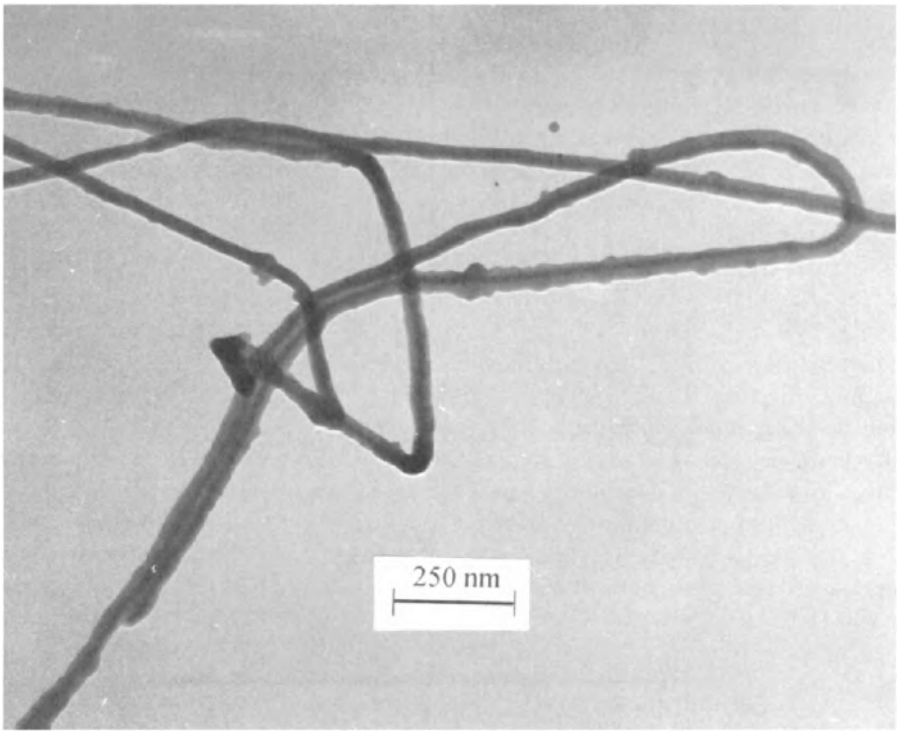

Fig. 15. Core–shell structure of S750-C107 nanofibers. The TEM sample was prepared by freeze-drying a benzene solution of nanofibers on a copper grid. (Source: Reprinted with permission from [73]. © 1996 American Chemical Society.)

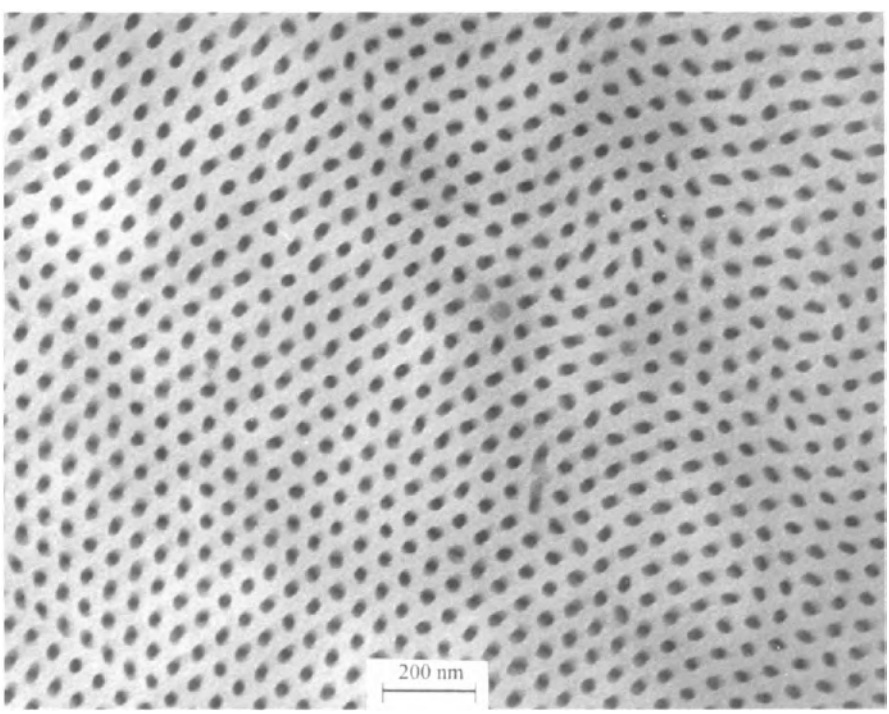

Fig. 16. Ordered domain structure of S750-C107 in bulk. The dark regions represent PCEMA cylinders pointing out of the picture.

8.2. Potential Applications

Since microdomain formation occurs in most block copolymers, it represents a general method for preparing uniform nanofibers from polymers with various diameters. We expect this method to be useful in producing precursor fibers that can be pyrolyzed to yield carbon or metal carbide nanofibers. Alternatively, this method can be modified to make nanowires by replacing the core block with a conductive polymer. In such a case, the outer block will function as an insulating plastic layer.

The S750-C107 nanofibers were found to be soluble in bromoform at all mixing ratios. Illustrated in Figure 17 is a polarized optical microscopic image of a trace left in a 42.5%, by weight, S750-C107 nanofiber solution in bromoform, after a spatula stroke through the solution [77]. The birefringence suggests alignment of the fibers along the scratching direction. As the relative position between the polarizers and the sample stage changed, the bright regions in the image turned dark and vice versa, as expected. Although such nanofibers, particularly water-soluble nanofibers, may be useful as "environmentally friendly" liquid crystals, their sluggish response to changes in electric fields may ultimately limit their application in liquid crystal display applications. This remains to be established with a more detailed study. The liquid crystalline properties of the nanofibers would certainly facilitate the preparation of macroscopic ropes consisting of well aligned nanofibers or nanofilaments.

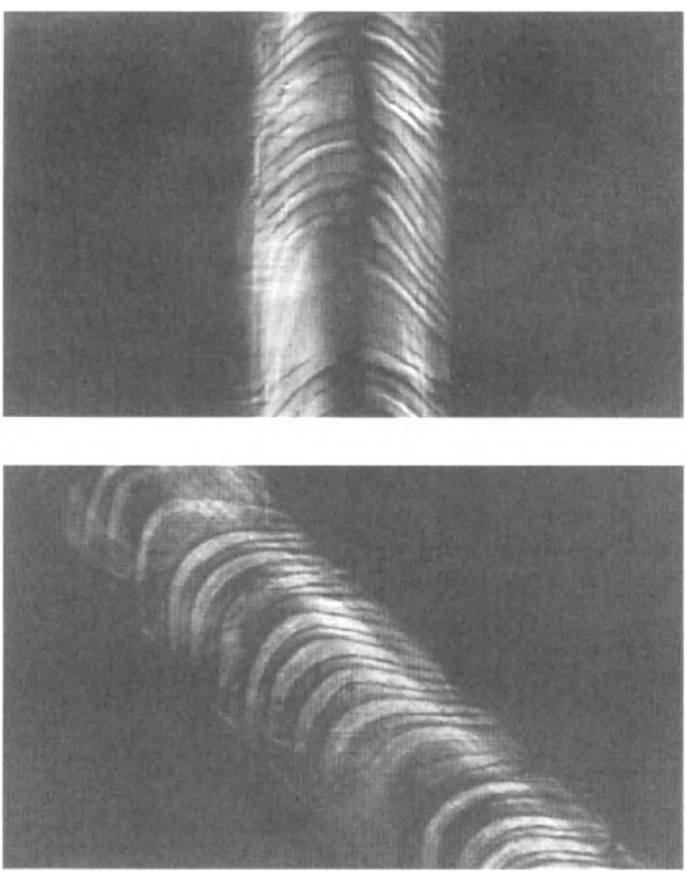

Fig. 17. Optical microscopic images of a trace left after a spatula stroke across a 42.5% by weight S750-C107 nanofiber solution in bromoform. The top picture was taken at a position with the shearing direction parallel to the analyzing polarizer axis. The bottom picture was taken after the sample stage was rotated by 45°. The width of each frame is about 5 mm.

9. NANOCHANNELS IN THIN FILMS

Individual nanotubes have been prepared from carbon [68, 78], peptides [79], and silica gel [80]. When the tubes are dispersed in a matrix, they are referred to as nanochannels. Nanochannels with a narrow size distribution but no regular packing were prepared in polymer films by the track-etch method [81–83]. More recently, methods have been developed for the formation of hexagonally packed nanochannels with narrow size distributions in metals [84, 85], glasses [86], zeolite particles [5], zeolite films [87], and even in a diblock solid [88]. No evaluation of thin films containing hexagonally packed nanochannels as membranes has been reported, however. In this section, a brief review of nanochannel preparation from one diblock copolymer and the performance of the thin film prepared as membranes [13, 89] will be given.

9.1. Example Membrane Preparation

The general procedure for membrane preparation from a diblock copolymer involves (1) synthesis of a diblock copolymer $(A)_n(B)_m$ with the A block degradable and the B block cross-linkable; (2) preparation of $(A)_n(B)_m$ solid with A forming the regularly packed cylinders dispersed in the continuous B matrix; (3) obtaining thin films of the diblock from microtomy; (4) cross-linking the continuous B phase; (5) full or partial degradation of the A cylinders [13].

We first prepared thin films with nanochannels from *t*380-C640 (P*t*BA-*b*-PCEMA with 3.8×10^2 units of *t*BA and 6.4×10^2 units of CEMA). At $n/m = 0.59$, P*t*BA formed cylinders dispersed in the PCEMA matrix. Slices with thickness between 0.050 and 2 μm were obtained by ultramicrotomy and irradiated with UV light that had passed through a 310-nm cutoff filter to obtain a PCEMA conversion of ~38%. The films were then supported on gold TEM grids and soaked in a 0.050-M $(CH_3)_3SiI$ solution in CH_2Cl_2 for 2 weeks to perform the following reaction in the P*t*BA cylinders:

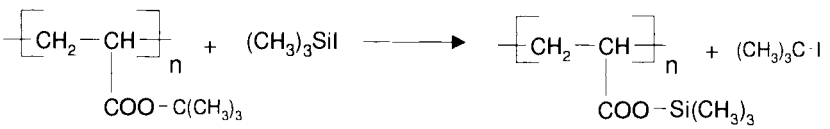

The trimethylsilyl groups were subsequently cleaved by hydrolysis in a water/methanol (v/v = 5/95) mixture. Upon drying, the poly(acrylic acid) chains should collapse to the PCEMA walls to yield thin films that contain nanochannels partially filled with PAA chains. Illustrated in Figure 18 is a TEM image of a small area of a 50-nm-thick film, where the light circles represent channels normal to the picture. Because the contrast between the light cylindrical domains and the dark PCEMA phase was obtained without chemical staining, the lighter regions should have lower polymer mass densities, as expected, due to the removal of the *t*-butyl groups [13]. The hexagonally packed channels in this case have a diameter of ~17 nm and a density of $\sim 5 \times 10^{10}/cm^2$.

9.2. Chemical Valving Effect

To test water permeation, a 2-μm-thick PS-*b*-PAA film was sandwiched between two polyethylene films (~30 μm thick) with paraffin linings (~10 μm thick), where both the polyethylene films and paraffin linings had a 1-mm hole in the center. The softer paraffin linings were used to obtain a seal between the polyethylene films and the membrane. After the membrane was sandwiched, the composite film was lightly pressed between two glass plates and mounted between two arms of a U-tube with a ground interface and a circular opening of ~1.5 mm. The two sides were held together by a clamp [89].

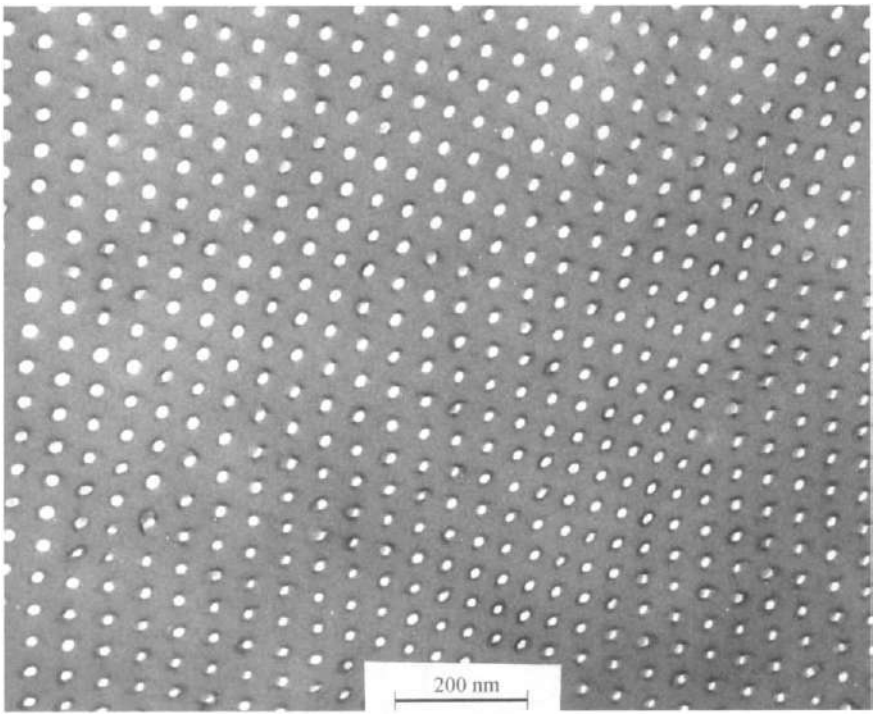

Fig. 18. TEM image of a small area of a 50-nm thick *t*380-C640 film. The PCEMA region of the film has been cross-linked and the *t*-butyl groups of the P*t*BA cylinders have been removed. (Source: Reprinted with permission from [17]. © 1997 American Chemical Society.)

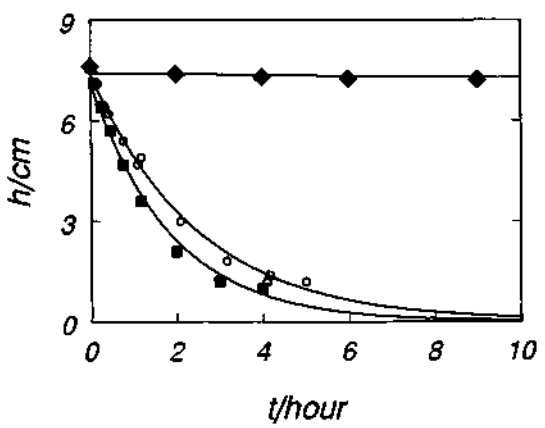

Fig. 19. Variation in the water height difference h between the two arms of a U-tube as a function of time t. The water transport rate was slowest at pH 3.0 (♦), but increased at pH 1.0 (○) and pH 13.0 (■).

Water flowed from one arm of a U-tube to the other due to a height difference of h between the two arms. Illustrated in Figure 19 is the variation in h with time t for aqueous solutions at three different pHs. The data were fitted with the equation

$$h = h_0 \exp(-t/\tau) \tag{2}$$

where h_0 is the initial height difference and $1/\tau$ is proportional to the membrane permeability constant P [90]. Plotted in Figure 20 is the variation in τ with pH (adjusted by adding

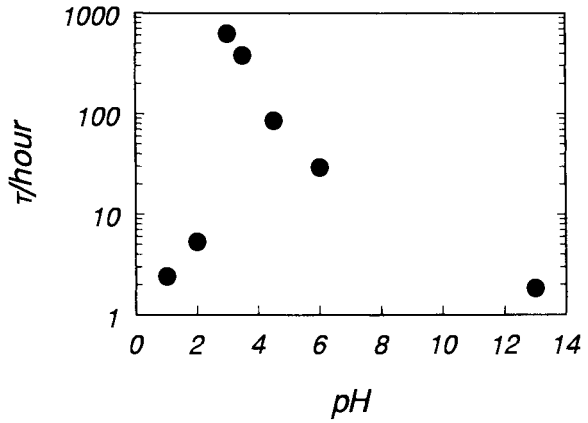

Fig. 20. Variation in τ as a function of pH.

different amounts of hydrochloric acid) for a membrane. The enormous variation in τ with pH demonstrates the tremendous potential of the nanochannels as "chemical valves" [89].

Water transportation rate is the lowest at pH ≈ 3, because the PAA chains take up little water and form a gel inside a nanochannel at this pH due to hydrogen bonding between different AA units [90]. As pH is decreased, the hydrogen bonds are broken by protons, which increases P. The P value increased at high pHs, because the AA groups are converted into sodium acrylate, which does not form hydrogen bonds easily. Also, ionized carboxyl groups take up more water molecules for solvation.

We also examined the effect of ionic strength on λ. At pH 6.0, the τ values were 29 and 10 h, respectively, in water and in an aqueous 0.100-M NaCl solution.

The effect of the divalent cation was demonstrated with the use of a 1.0-M $CaCl_2$ solution. When such a solution was used, the water height difference between the two sides of a U-tube remained at 7.6 cm after 28 h. This suggests the complete blockage of these nanochannels to water transportation. This closure was probably caused by Ca^{2+}-induced network formation from PAA because each Ca^{2+} ion may bind to two AA units of different PAA chains.

9.3. Potential Applications

The methodology used for PCEMA-*b*-PAA membrane preparation is general and can be used to prepare membranes from other diblocks. Like traditional membranes, membranes produced this way should have a wide range of applications. The potential advantage of membranes produced from this method may lie in their improved selectivity toward different permeates due to uniform pore size. These membranes also should work well as templates for further metal or semiconductor nanostructure fabrication. The particular PCEMA-*b*-PAA films prepared should be useful in sensing devices and controlled drug delivery, because the PAA channels close and open depending on their chemical environments. Also, the membranes should be useful in studying polymer chain reptation across nanochannels.

10. CONCLUDING REMARKS

The range of nanostructures we prepared is diversified. The underlying principle is, however, straightforward and involves (a) diblock self-assembly, (b) locking in the mesophasic structure by cross-linking one block, and possibly (c) the degradation of the other block.

The block copolymer nanostructures prepared may have applications not only in the general area of nanosized electronic device manufacturing, but also in fields such as catalysts, controlled drug delivery, water reclamation, separation science, nanocomposite preparation, etc. Although our work so far has been restricted to the use of diblock copolymers, the use of triblock copolymers in the future will further expand the repertoire of functional polymeric nanostructures.

Acknowledgment

Many postdoctoral fellows and students contributed to the work reviewed herein. Their contributions have been acknowledged by citing their publications. The Natural Sciences and Engineering Research Council of Canada is thanked for research grants, equipment grants, and an industrial oriented research grant to G. Liu as well as a strategic grant to V. I. Birss and G. Liu. The generous support provided by the Environmental Sciences and Technology Alliance of Canada and VX Optronics to G. Liu is also gratefully acknowledged.

References

1. G.-M. Chow and K. E. Gonsalves, "Nanotechnology—Molecularly Designed Materials," ACS Symposium Series, Vol. 622. American Chemical Society, Washington, DC, 1996.
2. L. M. Gan and C. H. Chew, in "Polymeric Materials Encyclopedia—Synthesis, Properties and Applications" (J. C. Salamone, ed.), p. 4321. CRC Press, Boca Raton, FL, 1996.
3. (a) H. Chen, K. Ishizu, T. Fukutomi, and T. Kakurai, *J. Polym. Sci., Polym. Chem.* 22, 2123 (1984); (b) K. Li and H. D. H. Stöver, *J. Polym. Sci., Polym. Chem.* 31, 3257 (1993).
4. C. R. Martin, *Science* 266, 1961 (1994).
5. (a) N. K. Raman, M. T. Anderson, and C. J. Brinker, *Chem. Mater.* 8, 1682 (1996); (b) J. S. Beck, J. C. Vartuli, W. J. Roth, M. E. Leonowicz, C. T. Kresge, K. D. Schmitt, C. T.-W. Chu, D. H. Olson, E. W. Sheppard, S. B. McCullen, J. B. Higgins, and J. L. Schlenker, *J. Am. Chem. Soc.* 114, 10834 (1992); (c) S. A. Bagshaw, E. Prouzet, and T. J. Pinnavaia, *Science* 269, 1242 (1995).
6. Y. H. Chiou, T. G. Tsai, H. C. Shih, C. N. Wu, and K. J. Chao, *J. Mater. Sci. Lett.* 15, 952 (1996).
7. Z. Tuzar and P. Kratochvil, *Surf. Colloid. Sci.* 15, 1 (1993).
8. A. Halperin, M. Tirrell, and T. P. Lodge, *Adv. Polym. Sci.* 100, 31 (1991).
9. J. Tao, A. Guo, and G. Liu, *Macromolecules* 29, 1618 (1996).
10. G. Liu, C. K. Smith, N. Hu, and J. Tao, *Macromolecules* 29, 220 (1996).
11. F. Henselwood and G. Liu, *Macromolecules* 30, 488 (1997).
12. M. E. Jung and M. A. Lyster, *J. Amer. Chem. Soc.* 99, 968 (1976).
13. G. Liu, J. Ding, A. Guo, M. Herfort, and D. Bazett-Jones, *Macromolecules* 30, 1851 (1997).
14. J. Ding and G. Liu, *Macromolecules* 30, 655 (1997).
15. R. Saito, K. Ishizu, and T. Fukutomi, *Polymer* 33, 1712 (1992); 31, 679 (1990).
16. Z. Tuzar, B. Bednar, C. Konak, M. Kubin, S. Svobodova, and K. Prochazka, *Makromol. Chem.* 182, 399 (1982).
17. D. J. Wilson and G. Riess, *Eur. Polym. J.* 24, 617 (1988).
18. (a) K. Ishizu and A. Onen, *J. Polym. Sci., Part A: Polym. Chem.* 27, 3721 (1989); (b) K. Ishizu and K. Kuwahara, *J. Polym. Sci., Part A: Polym. Chem.* 31, 661 (1993).
19. A. Guo, G. Liu, and J. Tao, *Macromolecules* 29, 2487 (1996).
20. J. Tao, S. Stewart, G. Liu, and M. Yang, *Macromolecules* 30, 2738 (1997).
21. S. Bywater, *Adv. Polym. Sci.* 30, 89 (1979).
22. J. Tao and G. Liu, unpublished data.
23. A. Halperin, *Macromolecules* 20, 2943 (1987).
24. P. G. de Gennes, in "Solid State Physics, Supplement 14" (J. Liebert, ed.). Academic Press, New York, 1978.
25. T. L. Bluhm and M. D. Whitmore, *Can. J. Chem.* 63, 249 (1985).
26. R. Xu, M. A. Winnik, G. Riess, B. Chu, and M. D. Croucher, *Macromolecules* 25, 644 (1992).
27. G. A. McConnell, A. P. Gast, J. S. Huang, and S. D. Smith, *Phys. Rev. Lett.* 71, 2102 (1993).
28. L. Oranli, P. Bahadur, and G. Riess, *Can. J. Chem.* 63, 2691 (1985).
29. M. Antonietti, S. Heinz, M. Schmidt, and C. Rosenauer, *Macromolecules* 27, 3276 (1994).
30. A. Qin, M. Tian, C. Ramireddy, S. E. Webber, P. Munk, and Z. Tuzar, *Macromolecules* 27, 120 (1994).
31. L. Zhang, R. J. Barlow, and A. Eisenberg, *Macromolecules* 28, 6055 (1995).
32. K. Khougaz, I. Astafieva, and A. Eisenberg, *Macromolecules* 28, 7135 (1995).

33. G. Wang, F. Henselwood, and G. Liu, *Langmuir* 14, 1554 (1998).
34. F. Henselwood, G. Wang, and G. Liu, *J. Appl. Polym. Sci.* 70, 397 (1998).
35. C. Sadron, *Pure Appl. Chem.* 4, 347 (1962).
36. J. Tao and G. Liu, *Macromolecules* 30, 2408 (1997).
37. V. A. Davankov, M. M. Ilyin, M. P. Tsyurupa, G. I. Timofeeva, and L. V. Dubrovina, *Macromolecules* 29, 8389 (1996).
38. L. Zhang and A. Eisenberg, *Science* 268, 1728 (1995).
39. J. Ding, G. Liu, and M. Yang, *Polymer* 38, 5497 (1997).
40. P. A. Canham, T. P. Lally, C. Price, and R. B. Stubbersfield, *J. Chem. Soc., Faraday Trans. 1* 55, 1857 (1980).
41. J. Ding and G. Liu, *Chem. Mater.* 10, 537 (1998).
42. J. Tao, G. Liu, J. Ding, and M. Yang, *Macromolecules* 30, 4084 (1997).
43. F. Li and G. Liu, research in progress.
44. S. Milner, *Science* 251, 905 (1991).
45. A. P. Gast, in "Scientific Methods for the Study of Polymer Colloids and Their Applications" (F. Landau and R. H. Otlewill, eds.). Kluwer Academic Publishers, Amsterdam, 1990.
46. G. Liu, in "The Polymeric Materials Encyclopedia—Synthesis, Properties, and Applications" (J. C. Salamone, ed.), p. 1548. CRC Press, Boca Raton, FL, 1996.
47. D. H. Napper, "Polymeric Stabilization of Colloidal Dispersions." Academic Press, London, 1983.
48. H. J. Taunton, C. Toprakcioglu, L. J. Fetters, and J. Klein, *Macromolecules* 23, 571 (1990).
49. H. Watanabe and M. Tirrell, *Macromolecules* 26, 6455 (1993).
50. E. Kumacheva, J. Klein, P. Pincus, and L. J. Fetters, *Macromolecules* 26, 6477 (1990).
51. M. Tirrell, in "Solvents and Self-Organization of Polymers" (S. E. Webber, P. Munk, and Z. Tuzar, eds.), NATO ASI Series E: Applied Sciences, Vol. 327. Kluwer, Dordrecht, 1996.
52. M. R. Munch and A. P. Gast, *Macromolecules* 23, 2313 (1990).
53. R. S. Venkatachalam, F. J. Boerio, P. G. Roth, and W. H. Tsai, *J. Polym. Sci., Part B: Polym. Phys.* 26, 2447 (1988).
54. P. P. Hong, F. J. Boerio, M. Tirrell, S. Dhoot, and P. Guenoun, *Macromolecules* 26, 3953 (1993).
55. W. H. Tsai, F. J. Boerio, M. Tirrell, and E. Parsonage, *Macromolecules* 24, 2538 (1991).
56. F. Bossé, H. P. Schreiber, and A. Eisenberg, *Macromolecules* 26, 6447 (1993).
57. E. Parsonage, M. Tirrell, H. Watanabe, and R. G. Nuzzo, *Macromolecules* 24, 1987 (1991).
58. C. Huguenard, R. Varoqui, and E. Pefterkron, *Macromolecules* 24, 2226 (1991).
59. J. M. Stouffer and J. McCarthy, *Macromolecules* 21, 1204 (1988).
60. C. Marques, J. F. Joanny, and L. Leibler, *Macromolecules* 21, 1051 (1988).
61. G. Liu, in "Organic Thin Films" (C. Frank, ed.), p. 178. ACS Symposium Series. American Chemical Society, Washington, DC, 1998.
62. J. Ding, J. Tao, A. Guo, S. Stewart, N. Hu, V. I. Birss, and G. Liu, *Macromolecules* 29, 5398 (1996).
63. J. Tao, A. Guo, S. Stewart, V. I. Birss, and G. Liu, *Macromolecules* 31, 172 (1998).
64. J. Ding, V. I. Birss, and G. Liu, *Macromolecules* 30, 1442 (1997).
65. J. Tao and G. Liu, unpublished results.
66. (a) P. M. Ajayan, O. Stephan, Ph. Redlich, and C. Collex, *Nature* 375, 564 (1995); (b) W. Han, S. Fan, Q. Li, and Y. Hu, *Science* 277, 1287 (1997).
67. (a) H. Dai, E. W. Wong, Y. Z. Lu, S. Fan, and C. M. Lieber, *Nature* 375, 769 (1995); (b) E. W. Wong, B. W. Maynor, D. B. Luke, and C. M. Lieber, *Chem. Mater.* 8, 2041 (1996).
68. A. Thess, R. Lee, P. Nikolaev, H. Dai, P. Petit, J. Robert, C. Xu, Y. H. Lee, S. G. Kim, A. G. Rinzler, D. T. Colbert, G. E. Scuseria, D. Tomanek, J. E. Fischer, and R. E. Smalley, *Science* 273, 483 (1996).
69. N. G. Chopra, R. J. Luyken, K. Cherey, V. H. Crespi, M. L. Cohen, S. G. Louie, and A. Zettl, *Science* 269, 966 (1995).
70. L. Qi, J. Ma, H. Cheng, and Z. Zhao, *J. Phys. Chem.* 101, 3460 (1997).
71. N. M. Rodriguez, M. S. Kim, and R. T. K. Baker, *J. Phys. Chem.* 98, 13108 (1994).
72. B. H. Kear and P. R. Strutt, *Naval Res. Rev.* 46, 4 (1994).
73. G. Liu, L. Qiao, and A. Guo, *Macromolecules* 29, 5508 (1996).
74. F. S. Bates and G. H. Fredrickson, *Annu. Rev. Phys. Chem.* 41, 525 (1990).
75. H. Hasegawa and T. Hashimoto, in "Comprehensive Polymer Science," Suppl. 2 (G. Allen, S. L. Aggarwal, and S. Russo, eds.), p. 497. Pergamon Press, London, 1996.
76. (a) A. K. Khandpur, S. Förster, F. S. Bates, I. W. Hamley, A. J. Ryan, W. Bras, K. Almdal, and K. Mortensen, *Macromolecules* 28, 8796 (1995); (b) M. W. Matsen and F. S. Bates, *Macromolecules* 29, 1091 (1996).
77. G. Liu, J. Ding, L. Qiao, A. Guo, B. P. Dymov, J. Gleeson, T. Hashimoto, and K. Saijo, *Chem.—Eur. J.*, in press.
78. S. Iijima, *Nature* 354, 56 (1991).
79. M. R. Ghadiri, in "Polymeric Materials Encyclopedia—Synthesis, Properties and Applications" (J. C. Salamone, ed.), p. 4888. CRC Press, Boca Raton, FL, 1996.
80. H. Nakamura and Y. Matsui, *J. Am. Chem. Soc.* 117, 2651 (1995).
81. R. L. Fleischer, P. B. Price, and R. M. Walker, "Nuclear Tracks in Solids." Univ. California Press, Berkeley, 1975.

82. M. Yoshida, M. Asano, A. Sagranj, H. Omichi, R. Spohr, J. Vetter, and R. Katakai, *Macromolecules* 29, 8987 (1996).
83. M. Nishizawa, V. P. Menon, and C. R. Martin, *Science* 268, 700 (1995).
84. H. Masuda and K. Fukuda, *Science* 268, 1466 (1995).
85. A. Despic and V. P. Parkhutik, in "Modern Aspects of Electrochemistry" (J. O. Bockris, R. E. White, and B. E. Conway, eds.), Vol. 20, p. 401. Plenum Press, New York, 1989.
86. D. H. Pearson and R. J. Tonucci, *Science* 270, 68 (1995).
87. (a) H. Yang, A. Kuperman, N. Coombs, S. Mamiche-Afara, and G. A. Ozin, *Nature* 379, 703 (1996); (b) H. Yang, N. Coombs, I. Sokolov, and G. A. Ozin, *Nature* 381, 589 (1996).
88. J.-S. Lee, A. Hirao, and S. Nakahama, *Macromolecules* 22, 2602 (1989).
89. G. Liu and J. Ding, *Adv. Mater.* 10, 69 (1998).
90. J. Hautojarvi, K. Kontturi, J. H. Nasman, B. L. Svarfvar, P. Viinikka, and M. Vuoristo, *Ind. Eng. Chem. Res.* 35, 450 (1996).